Probing the Spectral Function Using Momentum Resolved Radio Frequency Spectroscopy in Trapped Fermi Gases

Qijin Chen, and K. Levin

James Franck Institute and Department of Physics, University of Chicago, Chicago, Illinois 60637
(Dated: July 4, 2008)

We address recent momentum resolved radio frequency (RF) experiments on ultracold trapped Fermi gases of ^{40}K. We show that momentum resolved RF probes provide measurements of the centrally important fermionic spectral function. They also serve to remove ambiguity plaguing the interpretation of momentum integrated RF experiments by establishing a clear dispersion signature of pairing. We find that the temperature dependence of the spectral function is dramatic at unitarity, and, importantly, smooth from above to below T_c throughout BCS-BEC crossover. This should be tested experimentally, given widespread predictions of first order behavior.

Ultracold Fermi gases undergo BCS to Bose-Einstein condensation (BEC) crossover via a Feshbach resonance which is tuned with variable magnetic field. Study of BCS-BEC crossover has been argued [1] to be important for understanding high temperature superconductivity. These ultracold Fermi gases and their extensions to optical lattices are viewed as quantum simulators of some of the most important problems in condensed matter physics. However, due to the extreme small size of the Fermi gas cloud and the ultra low temperatures, the available experimental probes are limited by comparison with their condensed matter counterparts. Of particular importance are measurements of the fermionic spectral functions, $A(\mathbf{k},\omega)$ for which angle resolved photoemission spectroscopy (ARPES) has been so powerful in electronic systems. It is clear that counterpart experimental probes of $A(\mathbf{k},\omega)$, in the ultracold gases are crucial to progress.

Recent experiments on ^{40}K from the JILA group [2] have now demonstrated that it is possible to measure these spectral functions using momentum resolved RF pairing gap spectroscopy over a range of magnetic fields throughout the BCS-BEC crossover. There is a substantial advantage of using ^{40}K over the more widely studied ^{6}Li since, for the usual Feshbach resonance around 202 G, there are no nearby competing resonances to introduce complications from final state interactions. In this Letter we address the theoretical basis behind these measurements and demonstrate that this momentum resolved RF technique has, in principle, the same capabilities as that of ARPES. We then show that this technique can be used to shed light on the recent controversy [3] about the origin of double peak structure seen in previous [4] momentum-integrated RF spectra, as to whether it has to do with pairing or bound state effects. Both our calculations and the measurements in Ref. [2] of the momentum resolved RF spectral weight support the interpretation that a generic double peak structure in ^{40}K is associated with paired atoms near the trap center and unpaired atoms near the trap edge.

Importantly, we find that, near unitarity, the spectral function has a significant temperature variation. As in ARPES measurements of the temperature dependent spectral function these experiments can provide evidence for the presence of a normal state gap or pseudogap above T_c at unitarity. Indeed, a central focus of the cuprate literature has been to address the evolution of angle resolved photoemission experiments from above to below T_c. This focus provides the motivation for the present work, which addresses the counterpart to these experiments in the cold Fermi gases. Our work is based on a formalism that has been successfully applied to to ARPES measurements [5] in the high temperature superconductors. The corresponding physical picture of the pseudogap which opens at a temperature $T^* > T_c$ is that it arises from a stronger-than-BCS attraction leading to preformed, normal state pairs. The famous BCS paper highlights an additional challenge which must be met by theory: namely, explaining a smooth or *second order phase transition* at T_c. In the presence of BCS-BEC crossover we find that the transition should also be second order. This is at odds [6, 7] with widespread predictions of first order behavior in the literature.

In addressing RF spectroscopy we can ignore final state effects [8] for the particular resonance under consideration. In the recent JILA RF experiments [2] the momentum of state 3 atoms is measured using time-of-flight imaging, in conjunction with 3D distribution reconstruction. Since the 3D gas in a single trap is isotropic, detailed angular information is irrelevant. In a homogeneous system, the contributions to the RF current from state 2 to state 3 are of two types corresponding to transitions associated with the breaking of 1-2 pairs in the condensate or with the promotion of already existing thermal fermionic excitations to level 3. In RF transitions, a dominantly large fraction (Ω_L) of the photon energy $h\nu$ is used to excite the atoms in hyperfine level 2 to another internal state of the atom, corresponding to level 3, where Ω_L is the photon energy needed when the atoms in level 2 are free. By contrast, in the ARPES case, there is an "emission" process in that the photon energy is converted into the electron kinetic energy so that the electrons are knocked out of the crystal.

In the many-body theoretical derivation, it is convenient to choose the Fermi level of state 2 as zero energy, so that we define Ω_L' as the overall energy level splitting between the chemical potentials for atoms in level 3 and level 2. When pairing is present, the Green's function $G(K)$ for this state is gapped, and the Green's function $G_3^{(0)}(K)$ for state 3 is free.

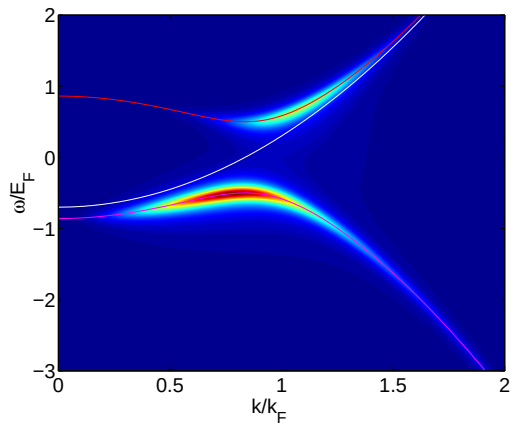

Figure 1: Contour plot of the occupied spectral intensity $A(k,\omega)f(\omega)k^2/2\pi^2$ at unitarity in the homogeneous case at $T/Tc \approx 1.9$. The three lines in the contour plots correspond to the two quasiparticle dispersions $\pm E_{\mathbf{k}}$ and the free atom dispersion, respectively, where we take $\mu = 0.7E_F$, $\Delta = 0.5E_F$, $T = 0.4T_F$, and $\gamma = 0.1E_F$.

We then have for the momentum-resolved RF current

$$\begin{aligned} I(\mathbf{k},\delta\nu) &= \frac{|T_k|^2}{(2\pi)^2}\int d\omega' A(\mathbf{k},\omega'-\Omega)A_3(\mathbf{k},\omega') \\ &\times \ [f(\omega)-f(\omega'+\Omega'_L)] \\ &= \frac{|T_k|^2}{2\pi}A(\mathbf{k},\omega)f(\omega)\Big|_{\omega=\epsilon_{\mathbf{k}}-\delta\nu} \end{aligned} \tag{1}$$

where $K \equiv (\mathbf{k}, i\omega_n)$ is the four-momentum, and $T_{\mathbf{k}}$ is the transition matrix element, which we will take to be a constant and then set to unity. This expression has been previously derived in Ref. [9], except there was also a momentum integral. We have also assumed that state 3 is essentially empty $[f(\omega'+\Omega'_L) = 0]$, and has a free dispersion $A_3(\mathbf{k},\omega) = 2\pi\delta(\omega-\epsilon_{\mathbf{k}}+\mu_3-\mu)$. Note here $\delta\nu = \Omega-\mu+\mu_3 = h\nu-\Omega_L$ is the RF detuning and $\omega = \epsilon_{\mathbf{k}}-\delta\nu$ is the energy of state 2 measured with respect to the Fermi level, where $\epsilon_{\mathbf{k}} = k^2/2m-\mu$, μ and μ_3 are the chemical potentials of atoms in state 2 and 3, respectively, and we take $\hbar = 1$. The last line of Eq. (1) is formally identical to the expression for ARPES signal intensity. In this way, it should be clear that momentum-resolved RF is equivalent to ARPES. Both measure the fermionic spectral function.

Beginning with Refs. 10 and 11, there have been studies of the spectral function associated with BCS-BEC crossover which show that, beyond the BCS regime, there is a spectral gap or pseudogap. Related work has also been performed by other groups [12]. Detailed numerical calculations [11] of the related normal state self energy (called Σ_{pg}) have led to a rather simple BCS-like form, which has been shown phenomenologically [13] to be quite successful for describing the normal phase of the cuprates. Following our earlier body of work [5, 9, 14] we presume that the self energy for a short-range interaction consists of a term arising from the condensed, Σ_{sc}, as well as noncondensed pairs (Σ_{pg}). We write $\Sigma(\mathbf{k},\omega) = \Sigma_{pg}(\mathbf{k},\omega)+\Sigma_{sc}(\mathbf{k},\omega)$, so that

$$\Sigma_{pg}(\mathbf{k},\omega) = \frac{\Delta_{pg}^2}{\omega+\epsilon_{\mathbf{k}}+i\gamma} - i\Sigma_0 \tag{2}$$

$$\Sigma_{sc}(\mathbf{k},\omega) = \frac{\Delta_{sc}^2}{\omega+\epsilon_{\mathbf{k}}}\,. \tag{3}$$

Here $\gamma \neq 0$ reflects a phenomenological broadening term, associated with a finite life time for incoherent pairs, and Σ_0 represents an "incoherent" background contribution, including that from the particle-hole channel. Σ_{sc} is associated with long-lived, condensed Cooper pairs and so it is of the same form as Σ_{pg} but without the broadening. With this self energy in the Green's functions, the resulting spectral function, $A(\mathbf{k},\omega) = -2\,\mathrm{Im}\,G(\mathbf{k},\omega+i0)$ can be readily determined. There is, moreover, a well defined procedure for computing the two contributions (from the condensed and noncondensed pairs) to the excitation gap which we do not repeat here. This formalism has been applied in the cold Fermi gas experiments [9, 15, 16, 17] as well as in the cuprate literature [5, 18].

In Fig. 1, we present an intensity map as a function of the single particle energy and the wave vector k for the states which contribute to the RF current in a homogeneous system. The yellow, red regions of the figure indicates those pairs of points (E,k) where the greatest number of contributing atoms lie. The temperature here is chosen to be relatively high, around $1.9T_c$ in order to have appreciable contributions to the RF current from pre-existing thermal fermionic excitations. The intensity map indicates upward and downward dispersing contributions. These correspond, to a good approximation, to the two RF transitions to state 3 from state 2 with dispersions $(E_{\mathbf{k}}+\mu)$ and $(-E_{\mathbf{k}}+\mu)$ relative to the bottom of the band. Here $E_{\mathbf{k}} = \sqrt{\epsilon_{\mathbf{k}}^2+\Delta^2}$ is the quasiparticle excitation energy, and $\Delta^2 = \Delta_{sc}^2+\Delta_{pg}^2$ defines the total gap Δ, with $\Delta_{sc} = 0$ above T_c. The width of the peaks in this contour plot comes exclusively from the incoherent terms γ and Σ_0. One can see that the bulk of the current even at this high temperature is associated with the pair states which are broken in the process of the RF excitation. This figure describes in a conceptual way, how this intensity map can be used to compare with a broadened BCS-like form for the spectral function, which fits very well the two branches shown in the figure corresponding to upward and downward dispersing curves. From the intensity map, one can determine the spectral gap by fitting the spectral function or the dispersion to a broadened BCS-like form, as has been done in Ref. [2].

We stress that the above calculations are for the homogeneous case and it is important to extend them to include the effects of a trap, where the density and gap reach maximum at the trap center and vanish at the trap edge. This is done within a local density approximation (LDA). Once the trap is included the simple analogy between the electronic ARPES experiments and momentum resolved photoemission spectroscopy is invalidated. While $\delta\nu$ is constant

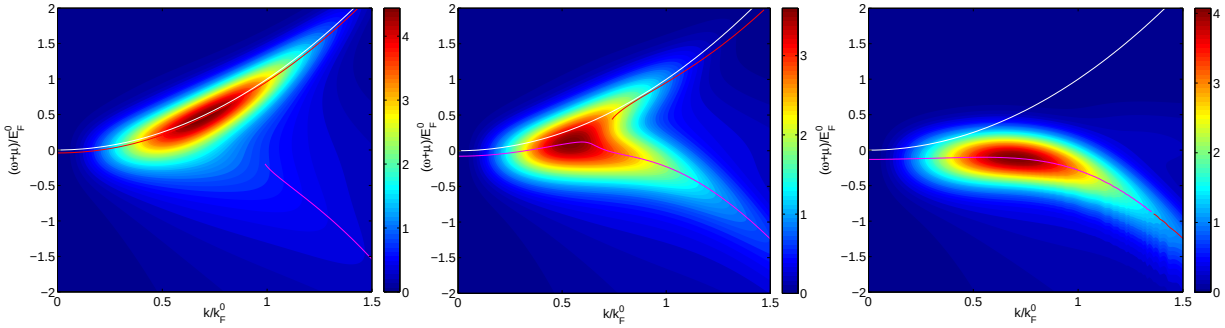

Figure 2: Contour plots of the occupied spectral intensity $A(k,\omega)f(\omega)k^2/2\pi^2 N$ at unitarity for (a) $T/T_c = 1.35$, (b) 0.8, and (c) 0.1, from left to right. Here $\Sigma_0 = 0.25E_F^0$ and $\gamma = 0.25(T/T_c)E_F^0$ at the trap center, and both scale with local density as r varies, $T_c \approx 0.27T_F^0$. The results were convoluted with a Gaussian broadening curve of width $\sigma = 0.22E_F^0$, whose value is taken from Ref. [2]. As T decreases, the spectral weight shifts from a free atom peak (upward dispersing curve) to a paired atom peak (downward dispersing curve). Here the lines indicate the loci of the peaks in the EDCs.

across the sample, the single particle excitation energy $\omega = k^2/2m - \mu(r) - \delta\nu$ will necessarily bear the inhomogeneity effect of the spatial dependence of $\mu(r)$; after time of flight imaging, one cannot distinguish atoms from different radii r. It is thus more convenient to measure the single particle energy from the band bottom, $\omega + \mu(r) = k^2/2m - \delta\nu$, which is constant across the trap for given k. Nevertheless, many of the central features survive. While in a homogeneous system there will be two branches as described above, in a trap, there is a third branch which appears as well. This corresponds to essentially free atoms at the trap edge which will contribute significantly to the RF current. This contribution dominates that of the thermally excited quasiparticles at both low and high T. It is this branch which is also upward dispersing and makes it rather difficult to see the contributions from pre-existing thermally broken pairs. With improved experimental resolution, this momentum resolved RF probe can in principle distinguish these two contributions by their dispersion.

The results of the LDA-based calculations for the intensity map plots are shown in Fig. 2 for the unitary gas in a trap, for different temperatures, calculated with $\Sigma_0 = \gamma = 0.25E_F^0$, and convoluted with an experimental Gaussian line of width $\sigma = 0.22T_F^0$. The vertical axis represents the trap averaged single particle energy, $(\omega + \mu)/E_F^0$, where $E_F^0 = (k_F^0)^2/2m$ is the global Fermi energy in the non-interacting limit. The temperatures are $T/T_c = 1.35$ (above T_c), 0.8 (slightly below T_c), and 0.1 (well below T_c), from left to right. At the highest T the central notable feature is a single upward dispersing curve which fits the free particle dispersion; the spectral weight is dominated by contributions from atoms at the trap edge. This dispersion can be readily differentiated from that associated with pre-existing thermally broken pairs which varies as $E_{\mathbf{k}} + \mu$ and of course, depends on the distribution of energy gaps $\Delta(r)$.

As the temperature decreases a second (downward dispersing) branch becomes evident. The spectral weight shifts to the lower branch gradually. The intensity map first bifurcates and eventually becomes dominated by the lower branch at very low T, where essentially all atoms are paired. Here the lower branch is associated with the breaking of a condensate pair. It, moreover, contains trap averaging effects. In the absence of final state effects, this can be used to determine the pairing gap. The separation of the two peaks can be difficult to discern until sufficiently high values of k.

That there are no abrupt changes at the superfluid transition distinguishes this theoretical scheme from others (e.g., Refs. [6, 7]) in the literature. Just as for the high temperature superconductors, there are no first order transitions as the system evolves from above to below T_c. The behavior at unitarity is in some sense smoother than in the strict BCS theory, since we find that a pairing gap is present above T_c, which shows up as a bifurcation in the intensity plots. There are indications [2] from the experimental momentum resolved RF plots that the behavior evolves smoothly from the normal to the superfluid phase, but detailed quantitative analyses to rule in or out possible first order transitions are lacking.

In Fig. 3A we plot the energy distribution curves (EDC) for a series of momenta k in a unitary trapped Fermi gas at $T/T_c = 1.1$ as a function of single particle energy. Here we have taken a somewhat larger intrinsic and instrumental broadening than in Fig. 1. These parameters are seen to optimize semi-quantitative agreement with the data. Thus the EDC in Fig. 3A can be compared with their counterparts plotted in Fig. 4 in Ref. [2]. At small k there is a single peak which separates into two at higher k values. The data are not sufficiently smooth to be assured that two peaks are visible at larger k, but they are consistent with this picture. As before, we attribute the separation at higher k to the fact that the upward and downward dispersing curves become most well separated in this regime. Better agreement is expected with improved signal-to-noise ratio in the data. Moreover, including detailed incoherent background contributions in the fermionic self-energy may also improve the agreement with experiment.

Figure 3B presents the corresponding spectral intensity map. The white dashed curve represents a fit of the experimental peak dispersion [2] while the solid white curve is the

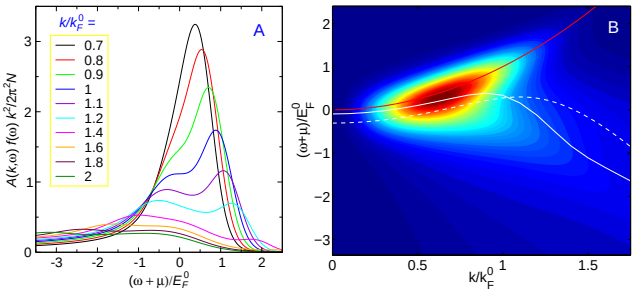

Figure 3: (A) Energy distribution curves for a series of momenta k as a function of single particle energy, and (B) corresponding occupied spectral intensity map, in a unitary trapped Fermi gas at $T/T_c = 1.1$. Here $\Sigma_0 = 0.35E_F^0$ and $\gamma = 0.38E_F^0$ at the trap center, and $\sigma = 0.3E_F^0$. In (B), the red curves represent the free atom dispersion, while the white solid and dashed curves are the quasiparticle dispersion obtained theoretically and experimentally [2], respectively, via fitting the EDCs with a single Gaussian distribution.

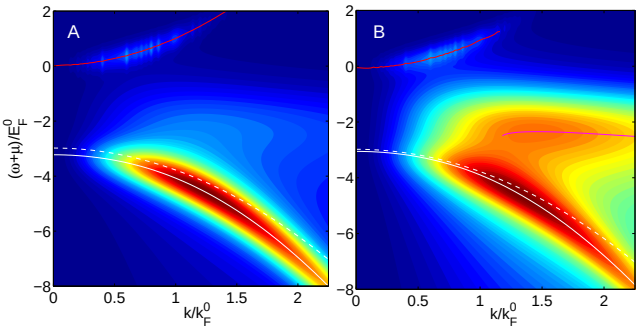

Figure 4: Occupied spectral intensity maps at $1/k_F^0 a = 1.1$ in the BEC case and $T/T_c = 1.3$. The broadening parameters at the trap center are $\Sigma_0 = 0.35E_F^0$ and $\gamma = 0.45E_F^0$ for the left panel and $\Sigma_0 = 1.0E_F^0$ and $\gamma = 1.3E_F^0$ for the right panel. For both, $\sigma = 0.25E_F^0$. Coherent sharp quasiparticle peaks can be seen in the left panel. Larger broadening in the right panel makes the coherent peak less pronounced, mimicking possible effects of chemical non-equilibrium. The red curve represents free atom dispersion, and the solid and dashed white curves represent the theoretical and experimental quasiparticle dispersion, respectively.

theoretical counterpart. Here, as in experiment we have fit the EDC to a *single* Gaussian peak. The comparison between the two white curves shows semi-quantitative consistency. Moreover, both the solid and dashed white curves can be well fit to the BCS dispersion involving $E_{\mathbf{k}}$, as was originally proposed in Ref. [10]. Indeed Fig. 3B seems to capture the essential results shown in Fig. 3a in Ref. [2]. With higher experimental resolution it should be possible to obtain more direct information about the mean gap size. In these experiments on ^{40}K, final state effects should be of less importance in complicating the interpretation. The fact that the experiments were done near T_c suggests that there is a sizable pseudogap at and above T_c at unitarity.

We turn finally to the BEC side of resonance in Fig. 4. Here the intensity map is presented for $1/k_F^0 a = 1.1$ at a temperature $T/T_c = 1.3$, where $T_c \approx 0.3T_F^0$. Even at this relatively high temperature there is virtually no weight in the free atom peak, associated with atoms at the trap edge. All the atoms are bound into pairs and there is only one downward dispersing peak in the plot. This behavior can be contrasted with that shown in Fig. 3c of Ref. [2] where there is a free atom contribution, which has been attributed to unpaired atoms out of chemical equilibrium with the pairs. In addition the downward dispersing peak in the left panel is rather sharp. In contrast, the large peak width in Ref. [2] seems to suggest incoherent contributions to the fermionic self energy, which may have to do with chemical non-equilibrium. The underlying theory here presumes that there are still well defined quasiparticles on the BEC side of resonance. We present in Fig. 3b the case in which we have considered a substantially larger intrinsic broadening $\gamma \approx \Delta$ to represent some of the qualitative features of the experimental data.

In conclusion, we have shown that momentum resolved RF spectroscopy can be used to measure the centrally important spectral function of ultracold Fermi gases. Other spectroscopic experimental tools have been proposed in the literature [19], although currently there are no counterpart experimental studies. We show that our calculated spectral intensity maps are in semi-quantitative agreement with experiments on ^{40}K. Because they establish the actual dispersion associated with the RF current contributions, these experiments remove ambiguity associated with whether pairing contributions might be confused with final bound state effects [3]. Both our theory and the experiments in Ref. [2] reveal that a double peak structure reminiscent of that seen in previous RF spectra [4] is indeed associated with paired atoms at the trap center and unpaired atoms at the trap edge. At unitarity, we show that there is substantial temperature variation in the spectral weight distribution. Theoretically, the spectral intensity maps and quasiparticle dispersion evolve smoothly with temperature across T_c. Whether first order transitions exist, as some have predicted, will require further experiments.

This work is supported by NSF PHY-0555325 and NSF-MRSEC Grant No. DMR-0213745. We thank Debbie Jin, Jayson Stewart and John Gaebler for many useful communications.

[1] A. J. Leggett, Nature Physics **2**, 134 (2006).
[2] J. T. Stewart, J. P. Gaebler, and D. S. Jin, arXiv: 0805.0026.
[3] C. H. Schunck, Y. Shin, A. Schirotzek, M. W. Zwierlein, and W. Ketterle, arXiv: 0802.0341.
[4] C. Chin, M. Bartenstein, A. Altmeyer, S. Riedl, S. Jochim, J. Hecker-Denschlag, and R. Grimm, Science **305**, 1128 (2004).
[5] Q. J. Chen and K. Levin, arXiv: 0712.1253.
[6] P. Pieri, L. Pisani, and G. C. Strinati, Phys. Rev. B **70**, 094508 (2004).
[7] R. Haussmann, W. Rantner, S. Cerrito, and W. Zwerger, Phys. Rev. A **75**, 023610 (2007).
[8] Y. He, C.-C. Chien, Q. J. Chen, and K. Levin, arXiv:0804.1429.
[9] Y. He, Q. J. Chen, and K. Levin, Phys. Rev. A **72**, 011602(R)

(2005).
[10] B. Jankó, J. Maly, and K. Levin, Phys. Rev. B **56**, R11407 (1997).
[11] J. Maly, B. Jankó, and K. Levin, Physica C **321**, 113 (1999).
[12] A. Perali, P. Pieri, G. C. Strinati, and C. Castellani, Phys. Rev. B **66**, 024510 (2002).
[13] M. R. Norman, A. Kanigel, M. Randeria, U. Chatterjee, and J. C. Campuzano, Phys. Rev. B **76**, 174501 (2007).
[14] Q. J. Chen, J. Stajic, S. N. Tan, and K. Levin, Phys. Rep. **412**, 1 (2005); K. Levin and Q. J. Chen, e-print cond-mat/0610006.
[15] J. Stajic, J. N. Milstein, Q. J. Chen, M. L. Chiofalo, M. J. Holland, and K. Levin, Phys. Rev. A **69**, 063610 (2004).
[16] J. Kinnunen, M. Rodriguez, and P. Törmä, Science **305**, 1131 (2004).
[17] Y. He, C.-C. Chien, Q. J. Chen, and K. Levin, Phys. Rev. A **77**, 011602(R) (2008).
[18] Q. J. Chen, K. Levin, and I. Kosztin, Phys. Rev. B **63**, 184519 (2001).
[19] T. L. Dao, A. Georges, J. Dalibard, C. Salomon, and I. Carusotto, Phys. Rev. Lett. **98**, 240402 (2007).